

Transport of charged colloids in a nonpolar solvent

Cite this: *Soft Matter*, 2013, **9**, 5173

Tina Lin,^a Thomas E. Kodger^b and David A. Weitz^{*ab}

In nonpolar solvents, surfactants stabilize charge through the formation of reverse micelles; this enables the dissociation of charge from the surfaces of particles, thereby charge-stabilizing particle suspensions. We investigate the dynamics of such charged particles by directly visualizing their motion across a microfluidic channel in response to an external electric field. The presence of the reverse micelles has a significant effect on particle motion: in a constant field, the particles initially move, then slow down exponentially, and eventually stop. This is due to the accumulation of reverse micelles at the channel walls, which screens the applied field, leading to the subsequent decay of the internal electric field. The time constant of decay depends on the electrical conductivity of the particle suspension and the width of the channel; this behavior is modeled as an equivalent RC circuit.

Received 28th February 2013
Accepted 8th April 2013

DOI: 10.1039/c3sm50619c

www.rsc.org/softmatter

Introduction

Polar environments have a low electrostatic barrier to charge dissociation; consequently, charge is ubiquitous and often plays an important practical role, as, for example, in the stabilization of colloidal dispersions. Electrostatic interactions in these dispersions are readily tuned through addition of salt.¹ By contrast, in nonpolar solvents, charges do not readily dissociate and charge-induced effects are typically not expected. Nevertheless, charge-induced effects are made possible through the addition of surfactants:^{2–5} in nonpolar solvents, surfactants aggregate to form reverse micelles, which can stabilize charge within their cores. Thus, reverse micelles solubilize charge, allowing for dissociation of charge from the surface of colloidal particles as well as stabilization of charge on the surface of the particles.^{3–12} This provides a mechanism to charge-stabilize colloidal suspensions in nonpolar environments that is very similar to that of polar environments. Particle suspensions charged with reverse-micelle-forming surfactants are central to a variety of applications,^{12,13} including electrophoretic displays, in which charged pigment particles are driven by an electric field to compose an image.¹⁴ In such applications, the ability to precisely control the trajectories and locations of charged particles with an electric field is essential. However, the electrical properties of charged particle suspensions are influenced by the reverse micelles in the bulk fluid,¹⁵ which not only stabilize the counter-charges but also stabilize additional charges, resulting in increased electrical conductivity and charge screening. Thus, reverse micelles can have an effect on the response of charged colloidal particles to an applied electric

field;¹⁶ however, the details of this scenario are not fully understood. Such knowledge is important for practical purposes, including the ability to predict and control charged particle behavior; it is also essential for gaining a better understanding of the electrodynamic properties of such systems. This requires a detailed investigation of charged particle motion in nonpolar solvents and the influence of reverse micelles on this motion.

Here, we investigate the dynamics of colloidal particles suspended in a nonpolar solvent and charged through the addition of reverse micelles by directly visualizing their motion across a microfluidic channel in response to an applied electric field. We find that the presence of the charged reverse micelles has a significant effect on particle transport: in a constant applied electric field, the colloidal particles initially move, but then unexpectedly slow down and stop. We show that this transport behavior is due to a buildup of charged reverse micelles, which subsequently screen the applied field. As a result, the internal electric field within the channel decays exponentially in time; the decay behavior depends on the conductivity of the suspension and the size of the channel. This system is modeled as an equivalent RC circuit.

Experimental

We synthesize 1 μm diameter, fluorescently labeled poly(methyl methacrylate) (PMMA) colloidal particles.¹⁷ Methyl methacrylate and methacrylic acid monomers, dimethylacrylate–polydimethylsiloxane stabilizer (Gelest DMS-R31), BODIPY 543 fluorophore, AIBN initiator, and hexane solvent are placed in a flask and heated to 80 °C under reflux for 6 hours. The particles are cleaned and resuspended in decalin at a volume fraction of 0.1%. The presence of methacrylic acid in the polymer particle allows for a negatively charged ionizable group. The particles

^aDepartment of Physics, Harvard University, 17 Oxford St., Cambridge, MA 02138, USA. E-mail: weitz@seas.harvard.edu

^bSchool of Engineering and Applied Science, Harvard University, 29 Oxford St., Cambridge, MA 02138, USA

also have polydimethylsiloxane (PDMS) brushes on their surfaces which provide steric stabilization.

We use aerosol-OT (AOT, or sodium di-2-ethyl-hexylsulfosuccinate) as the charge control agent in our particle suspensions; AOT is a surfactant with a polar head and two nonpolar hydrocarbon tails. In nonpolar solvents, AOT forms reverse micelles with a radius on the order of 1 nm. A fraction of the AOT reverse micelles are charged; these typically contain a single charge. Even though the reverse micelles have less charge than the particles, they are much smaller in size; therefore, the mobility of charged reverse micelles is typically at least an order of magnitude larger than that of the charged particles.

After adding AOT to a particle suspension, we allow the suspension to equilibrate for at least 1 day and sonicate it to ensure a homogeneous dispersion. The conductivity of the particle suspensions is measured with a Scientifica 627 conductivity meter.

To investigate the motion of the particles, we use a microfluidic device that allows us to apply an electric field across the particle suspension and directly observe the most important dimension: the plane consisting of the field lines and particle motion. The microfluidic device is fabricated with Norland Optical Adhesive (NOA 81).¹⁸ The device consists of three parallel channels which are separated by a 10 μm -wide wall and all of the channels are 25 μm -high. The two outer channels are filled with a low-temperature solder (Indium Corporation), forming two parallel electrodes, as shown in Fig. 1. The width of each of the electrodes is 100 μm , while the width of the central channel is varied for different devices. The central channel is filled with the particle suspension, and then sealed with epoxy.

The electrodes are connected in series to a function generator (Agilent 33250A) and a high-voltage amplifier (Trek 2210). We apply and repeatedly reverse a voltage difference across the particle suspension; as a result, the charged particles move back and forth across the channel. We image the particles using a confocal microscope (Leica SP5). As the particles move in response to a reversal in the applied field, we capture sequential images at rates of up to 200 frames per second; these images are used to track the locations of the particles. We wait several seconds between each reversal; this allows us to capture the full range of particle motion, as most of the motion occurs within a timeframe on the order of 10–100 ms.

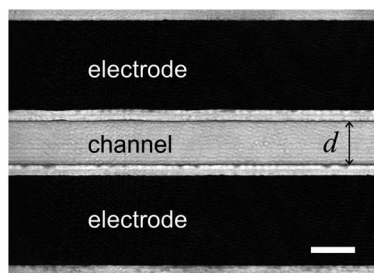


Fig. 1 Microfluidic device consisting of a channel of width d and two parallel electrodes. A thin wall separates each electrode from the channel. The scale bar is 50 μm .

Results and discussion

We visualize a particle suspension without any AOT within a 50 μm -wide channel: in response to an applied constant voltage of 10 V, the particles move towards the negative electrode, indicating that they are positively charged. The particles move until they contact the channel wall, whereupon they remain stationary. When the polarity of the applied field is reversed, the particles move in the opposite direction as they did before; they are transported completely across the channel until they reach the opposite wall, whereupon they again remain stationary. Particle motion is primarily in the direction perpendicular to the electrodes, along the electric field lines; additionally, the particles appear to move at a constant velocity across the channel. Images of particle transport are shown in Fig. 2(a). That these particles are charged even in the absence of any added charge control agent is surprising. Moreover, based on the particle synthesis procedure, the sign of the charge on these particles is unexpected. It is possible that the source of charge is due to trace contaminants; however, this charging behavior is reproducible.

To further analyze the motion of these particles, we track each individual particle as it moves across the channel after the polarity of the applied field is reversed. We focus on the primary direction of motion: in the direction of the applied field. Particle trajectories along this direction are linear in time, as shown in Fig. 2(b); this indicates that the velocity of each particle as it travels across the channel is indeed constant. For different applied voltages, we measure the individual particle trajectories and average them: the particles move across the channel faster

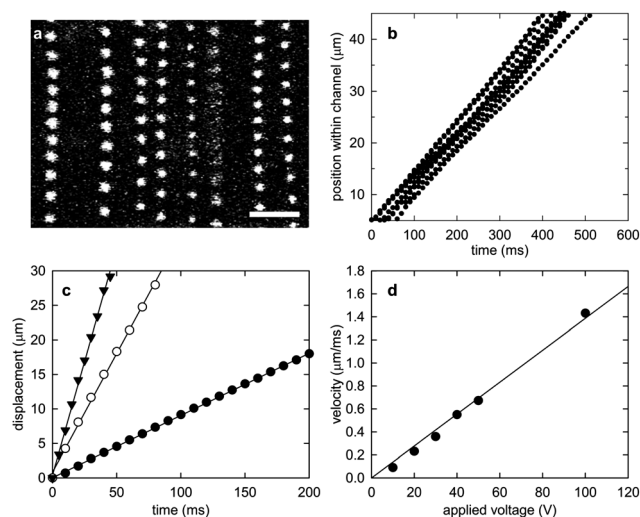


Fig. 2 Transport of particles with no AOT across a channel of width $d = 50 \mu\text{m}$ in response to a reversal in the applied voltage. (a) 15 superimposed consecutive images of particles moving across an area within the channel; the applied voltage is 10 V. The electrodes are located above and below the pictured area; the particles move from top to bottom. The time between each image is 18 ms. The scale bar is 10 μm . (b) Particle locations along the direction of the applied field; the applied voltage is 10 V. (c) Average particle displacements and linear fits for different applied voltages: 10 V (filled circles), 30 V (open circles), and 50 V (triangles). (d) Average particle velocity as a function of applied voltage; the line is a linear fit.

as the voltage is increased, as shown in Fig. 2(c). The particle velocity, v , is obtained from the slope of the linear fit of the average particle trajectory; it increases linearly with the applied voltage as shown in Fig. 2(d). Since the applied field, E_A , is the applied voltage divided by the distance between electrodes, we can determine the electrophoretic mobility, μ , from $v = \mu E_A$; we find that $\mu = 9.73 \times 10^{-10} \text{ m}^2 \text{ V}^{-1} \text{ s}^{-1}$. By assuming that particle charge, Q , is related to mobility by $Q = 6\pi\eta\mu a$, where η is the liquid viscosity and a is the particle radius, we find that these particles have about 170 elementary charges.

When we add AOT to the solution, hence adding additional charges, we observe drastically different behavior. In response to a reversal of the applied constant voltage of 10 V, the particles in the suspension, to which we have added 10 mM AOT, initially move along the direction of the applied field, but then slow down and stop before arriving at the channel wall. Despite the continuously applied voltage, the particles no longer accumulate at the channel wall. When the polarity of the applied field is reversed, the particles move in the opposite direction, but then again slow down and stop before they contact the wall; images of particle transport are shown in Fig. 3(a). The measured trajectories of these particles along the direction of the applied field are nonlinear in time, as shown in Fig. 3(b). Furthermore, the initial movement of these particles is towards the positive electrode, indicating that the charge has reversed and they are now negatively charged. We had previously found that, without AOT, the particles are positively charged; similar charge sign reversal upon the addition of charge control agents has also been observed with other nonpolar particle systems.⁹

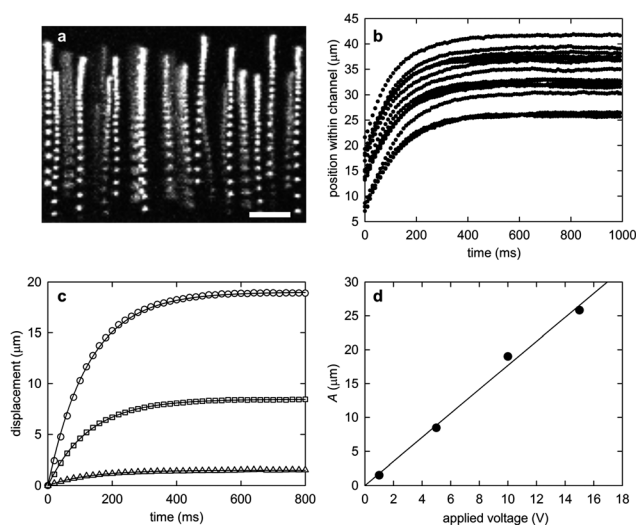


Fig. 3 Transport of particles with 10 mM AOT across a channel of width $d = 50 \mu\text{m}$ in response to a reversal of the applied voltage. (a) 30 superimposed consecutive images of particles moving within the channel when the applied voltage of 10 V is reversed. The electrodes are located above and below the pictured area; the particles move from bottom to top. The time between each image is 18 ms. The scale bar is $10 \mu\text{m}$. (b) Particle locations along the direction of the applied field; the applied voltage of 10 V is reversed at time $t = 0$. (c) Average particle displacements for different applied voltages: 10 V (circles), 5 V (squares), 1 V (triangles). The solid lines are fits to the exponential function $A(1 - \exp(-t/\tau))$. (d) The total distance traveled by the particles, A , as a function of the applied voltage; the line is a linear fit.

The nonlinear transport behavior is observed over a range of applied voltages, as shown in Fig. 3(c). We apply voltages that are large enough to induce visually discernable particle motion, yet small enough such that the particles do not reach the channel wall; this enables us to track the full range of particle motion. While the particles always move, slow down, and then stop, the distance they travel is dependent on the applied voltage. To quantify this behavior, we fit the average particle trajectories to an exponential function, $A(1 - \exp(-t/\tau))$, where the magnitude, A , corresponds to the distance traveled by the particles and the time constant, τ , corresponds to the decay of particle motion in time. We find that A grows linearly as a function of applied voltage, as shown in Fig. 3(d). By contrast, τ does not change with voltage; this is shown in Fig. 4(a).

We observe similar particle behavior as we vary the AOT concentration, or as we vary the channel widths; in an applied constant voltage, the particle motion decays in time. The decay time constant does not depend on the applied voltage; however, τ decreases as the AOT concentration is increased and τ increases with channel width, as shown in Fig. 4(a). In general, larger voltages are required for larger AOT concentrations; this may be in part due to the increase in the amount of charged species in the solution when AOT is added. To determine the amount of charged species, we measure the electrical conductivity of the particle suspension; it increases approximately linearly with AOT concentration, as shown in Fig. 4(b). Clearly, the motion of particles with AOT differs significantly from the motion of particles without AOT; thus, the reverse micelles must play an important role. When a constant field is applied across the channel, the charged particles and the charged reverse micelles move in response. The charged reverse micelles have a higher mobility than the particles; thus, they travel faster through the fluid and arrive at the channel walls sooner. The positively and negatively charged reverse micelles accumulate at opposite channel walls. These reverse micelles induce an electric field across the channel in the direction opposite to that of the applied field; consequently, the internal electric field, which is the superposition of the applied field and the induced field, is decreased. As a result, the charged species in the bulk slow down. Eventually, the buildup of charged reverse micelles is

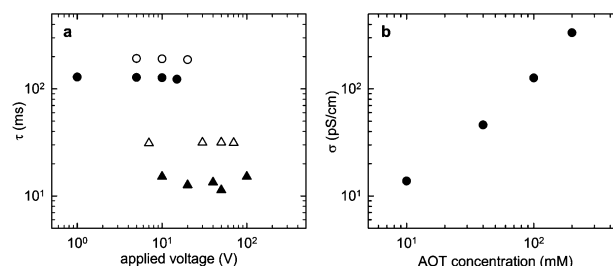


Fig. 4 (a) Time constants, τ , of decay of particle motion at different applied voltages for different AOT concentrations: 10 mM (circles) and 100 mM (triangles), and different channel widths: $50 \mu\text{m}$ (filled symbols) and $100 \mu\text{m}$ (open symbols). The time constant is independent of applied voltage. (b) Conductivity, σ , of the particle suspension versus AOT concentration. The dependence is roughly linear.

sufficiently large enough to completely neutralize the applied field; at this point, the colloidal particles stop moving entirely.

To determine how the internal electric field is affected by the charged reverse micelles, we consider the rate of their accumulation at the channel walls. The current density within the bulk, j , is given by $j = \sigma E^*$, where σ is the suspension conductivity and E^* is the internal field. The internal field is initially equal to the applied field, E_A . From the current density, we determine the rate of accumulation of charge per unit area, q , at either wall: $dq/dt = j = \sigma E^*$. The field induced by the accumulated reverse micelles, E_m , reduces the internal field: $E^* = E_A - E_m$. The applied field is held constant; therefore, the change in the internal field is $dE^*/dt = -dE_m/dt = -(1/d)dV_m/dt$, where V_m is the total voltage drop across the accumulated reverse micelles at both walls and d is the width of the channel. Since V_m is proportional to the amount of charge accumulated at the walls, $dE^*/dt \sim -(1/d)\sigma E^*$. The solution to this expression is $E^* = E_0 \exp(-t/\tau)$, where E_0 is E^* at $t = 0$ and $\tau \sim d/\sigma$ is the decay time constant. The exponential form of this internal field is consistent with the observed particle motion.

We also predict that τ is independent of the applied field; this is consistent with our observations of particle motion. In addition, we explicitly predict that $\tau \sim d/\sigma$. To test this prediction, we measure the average τ over the applied voltages as we vary the channel width and suspension conductivity. We indeed find that the average time constant varies linearly with d/σ , as shown in Fig. 5. This confirms our prediction and supports our picture that the decay of the internal electric field is due to the accumulation of charged reverse micelles.

The accumulation of charge at an electrode upon application of an external field is reminiscent of an electrochemical cell. This can be modeled as an RC circuit:^{15,19,20} the equivalent circuit consists of a resistor, the suspension, connected in series with two capacitors, the two interfaces. In an electrochemical cell, the resistance is $R = d/\sigma$ and the capacitance of each interface is $C = \epsilon/\lambda$, where ϵ is the dielectric constant of the solution and λ is the Debye screening length. The total capacitance for the two interfaces in series is $C/2$. The screening length scales as $\sigma^{-1/2}$,⁴ thus, the RC time constant is $\tau = d/\sigma \times \epsilon/2\lambda \sim d/\sigma^{1/2}$. By contrast, our measurement shows that time constant scales as d/σ . To explain this behavior, we consider the details of our microfluidic

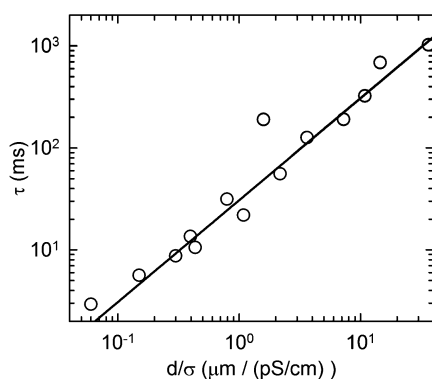


Fig. 5 Decay time constant as a function of d/σ . The line is a linear fit.

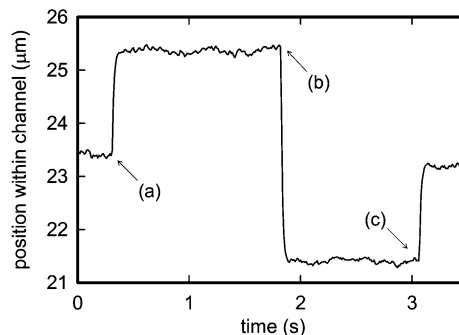


Fig. 6 Average particle trajectory when the applied voltage is (a) turned on from 0 to 30 V, (b) reversed, then (c) turned off to 0 V. The AOT concentration is 40 mM and d is 50 μm .

device: there is a wall of NOA separating each metallic electrode from the electrolyte; to account for these walls, the capacitance of each interface becomes $\epsilon/(\lambda + w)$, where $w = 10 \mu\text{m}$ is the width of the wall. The typical value of λ in nonpolar systems is on the order of 100 nm to 1 μm , at least an order of magnitude smaller than w ; therefore, the capacitance is dominated by the wall thickness, and is a constant. The resultant time constant thus varies as d/σ , in direct agreement with our measurements.

After the reverse micelles have completely screened the applied field and the particles have stopped moving, the internal field is $E^* = E_A - E_m = 0$. At this point, the field induced by the reverse micelles is equal in magnitude to the applied field, $E_m = E_A$, but in the opposite direction. When the applied field is reversed, it is then in the same direction as the induced field; at this point, the magnitude of the internal field is actually twice that of the applied field: $E^* = E_A + E_m = 2E_A$. Therefore, the particles travel twice as fast and twice as far compared to how they would if the field was turned on from 0. Similarly, if the applied field is turned off after complete screening, going from E_A to 0, the field induced by the micelles still remains: $E^* = -E_A$. Thus, the particle motion when the field is turned off is the same but in the opposite direction as when the field is turned on. We observe such particle behavior when the field is turned on, reversed, and then turned off, as shown in Fig. 6; in addition to causing the decay in particle motion in a constant field, the accumulated reverse micelles have a major effect on the particle motion when the applied field is then changed. This behavior is relevant for electrophoretic displays, in which the applied electric field is frequently and repeatedly reversed as well as turned on and off; the image quality must be maintained through these changes in the applied field.

Conclusions

Here, we find that the presence of charged AOT reverse micelles has a significant effect on the transport of charged particles in a nonpolar solvent. Through direct visualization of the motion of the charged particles, we are able to probe the internal electric field across the suspension. Despite a constant applied electric field, the internal electric field decays exponentially in time; this is due to the accumulation of charged AOT reverse micelles at

the channel walls which screens the applied field. This does not occur for particle suspensions without any AOT because the relatively low amount of charge in the solution is too small to significantly affect the internal field. The screening effect poses an important challenge for electrophoretic display technology, as surfactants similar to AOT are commonly used to stabilize charge in nonpolar particle dispersions. Our investigation of the dynamics of charged particles in a nonpolar solvent in an applied electric field provides a basis for the further investigation of methods to eliminate or overcome any undesired effects of charged reverse micelles on charged particle transport.

Acknowledgements

We thank E. Russell for the particle tracking code and R. Guerra for useful discussions. T.L. acknowledges support by the National Science Foundation Graduate Research Fellowship (DGE-1144152) and the Department of Defense (DoD) through the National Defense & Engineering Graduate (NDSEG) Fellowship Program. This work was also supported by the Harvard MRSEC (DMR-0820484) and the NSF (DMR-1006546).

Notes and references

- 1 E. R. Russell, J. Sprakel, T. E. Kodger and D. A. Weitz, *Soft Matter*, 2012, **8**, 8697.
- 2 Q. Guo, V. Singh and S. H. Behrens, *Langmuir*, 2010, **26**, 3203.
- 3 I. D. Morrison, *Colloids Surf., A*, 1993, **71**, 1.
- 4 M. F. Hsu, E. R. Dufresne and D. A. Weitz, *Langmuir*, 2005, **21**, 4881.
- 5 S. K. Sainis, J. W. Merrill and E. R. Dufresne, *Langmuir*, 2008, **24**, 13334.
- 6 C. E. Espinosa, Q. Guo, V. Singh and S. H. Behrens, *Langmuir*, 2010, **26**, 16941.
- 7 Q. Guo, J. Lee, V. Singh and S. H. Behrens, *J. Colloid Interface Sci.*, 2013, **392**, 83.
- 8 G. S. Roberts, R. Sanchez, R. Kemp, T. Wood and P. Bartlett, *Langmuir*, 2008, **24**, 6530.
- 9 G. N. Smith and J. Eastoe, *Phys. Chem. Chem. Phys.*, 2013, **15**, 424.
- 10 S. M. Hashmi and A. Firoozabadi, *Soft Matter*, 2012, **8**, 1878.
- 11 J. W. Merrill, S. K. Sainis and E. R. Dufresne, *Phys. Rev. Lett.*, 2009, **103**, 138301.
- 12 K. E. Tettey, M. Q. Yee and D. Lee, *Langmuir*, 2010, **26**, 9974.
- 13 V. Novotny, *Colloids Surf.*, 1987, **24**, 361.
- 14 B. Comiskey, J. D. Albert, H. Yoshizawa and J. Jacobson, *Nature*, 1998, **394**, 253.
- 15 M. Karvar, F. Strubbe, F. Beunis, R. Kemp, A. Smith, M. Goulding and K. Neyts, *Langmuir*, 2011, **27**, 10386.
- 16 F. Strubbe, F. Beunis, M. Marescaux, B. Verboven and K. Neyts, *Appl. Phys. Lett.*, 2008, **93**, 254106.
- 17 S. M. Klein, V. N. Manoharan, D. J. Pine and F. F. Lange, *Colloid Polym. Sci.*, 2003, **282**, 7.
- 18 D. Bartolo, G. Degre, P. Nghe and V. Studer, *Lab Chip*, 2007, **8**, 274.
- 19 M. Z. Bazant, K. Thornton and A. Ajdari, *Phys. Rev. E: Stat., Nonlinear, Soft Matter Phys.*, 2004, **70**, 021506.
- 20 D. C. Prieve, J. D. Hoggard, R. Fu, P. J. Sides and R. Bethea, *Langmuir*, 2008, **24**, 1120.